ICSV13 - Vienna
The Thirteenth International Congress on Sound and Vibration
Vienna, Austria, July 2-6, 2006

ACTIVE VIBRATION CONTROL OF A SLENDER CANTILEVER USING DISTRIBUTED PIEZOELECTRIC PATCHES

Manfred Nader*[1], Manfred Kaltenbacher[2], Michael Krommer[3], Hans-Georg von Garssen[4], Reinhard Lerch[2]

[1]Linz Center of Mechatronics GmbH,
Altenbergerstrasse 69, A-4040 Linz, Austria
[2]Department of Sensor Technology, Friedrich-Alexander-University Erlangen-Nuremberg,
Paul-Gordan-Strasse 3/5, D-91052 Erlangen, Germany
[3]Institute for Technical Mechanics, Johannes Kepler University Linz,
Altenbergerstrasse 69, A-4040 Linz, Austria
[4]Siemens AG Munich, CT PS 8,
Otto-Hahn-Ring 6, D-81729 Munich, Germany
manfred.nader@lcm.at

Abstract
In the present paper the concept of dynamic shape control is applied to compensate disturbing flexural vibrations in a cantilever beam. The idea of dynamic shape control is used to eliminate flexural vibrations, which arise due and in addition to a given support motion. For feedback control a collocated actuator and sensor design is proposed. The continuous distribution, derived from the method of dynamic shape control, is approximated by a finite number of piezoelectric patches. The controller itself is incorporated into our finite element software tool, which allows the full simulation of controlled piezoelectric structures.

INTRODUCTION

In many engineering applications vibrations are responsible for the generation of acoustic noise. Especially slender or thin-walled structures with a large surface contribute to this unwanted radiation. In the present paper the concept of dynamic shape control is applied to compensate the emerging disturbing vibrations. The goal of shape control is to eliminate structural deformations by means of a distributed control actuation. Thus, the spatial distribution of the actuation, together with its time evolution, is prescribed, such that the total

displacement field vanishes throughout the entire structure. The basic idea is derived for the case of a slender cantilever. For corresponding studies on beam vibrations, see e.g. Irschik, Krommer and Pichler [1], and for an application to plate vibrations, see Nader et al. [2]. Due to the prescribed support motion, flexural vibrations are emerging in addition to the rigid body motion. A continuous distribution for the piezoelectric actuation is derived analytically, which is able to eliminate the flexural vibrations of the beam. For practical feasibility the continuous actuation is approximated by distributed piezoelectric patches. The appropriate locations for the actuators as well as for the sensors are determined by finite element computations. A PD-controller using collocated actuators and sensors is designed and simulated within the environment of MATLAB/Simulink. The performance of the controller is evaluated by applying our finite element software tool, which allows the full simulation of controlled piezoelectric structures.

DYNAMIC SHAPE CONTROL

We study a slender cantilever beam of length L with a span-wise constant bending stiffness D and a span-wise constant linear inertia μ. At $x = 0$ the slope is prescribed zero, but a support motion $\overline{w}(t)$ is imposed. At $x = L$ homogenous dynamical boundary conditions are prescribed. Along the span of the beam no transverse forces are applied, but we consider an arbitrarily distributed eigenstrain-type moment $M^*(x,t)$ be applicable. We decompose the total deflection of the beam into two parts according to $w_0(x,t) = \overline{w}(t) + \Delta w(x,t)$, in which $\Delta w(x,t)$ characterizes the deviation of the total deflection from the rigid body motion, which follows the time variation of the support motion. The governing equations for this latter deviation of the deflection are

$$\begin{aligned} & D\Delta w_{,xxxx}(x,t) + \mu\Delta\ddot{w}(x,t) = -\left[\mu\ddot{\overline{w}}(t) + M^*_{,xx}(x,t)\right] , \\ & x = 0: \quad \Delta w = 0 \quad \text{and} \quad \Delta w_{,x} = 0 , \\ & x = L: \quad D\Delta w_{,xx} + M^* = 0 \quad \text{and} \quad D\Delta w_{,xxx} + M^*_{,x} = 0 , \end{aligned} \tag{1}$$

see e.g. Ziegler [3]. From Eq. (1) we establish an equation for the balance of that part of the kinetic energy that is solely due to the deviation of the deflection from the support motion. This balance equation reads

$$\begin{aligned} & \frac{\mathrm{d}}{\mathrm{d}t}\left[\frac{1}{2}\int_0^L \mu\Delta\dot{w}\Delta\dot{w}\mathrm{d}x + \frac{1}{2}\int_0^L D\Delta w_{,xx}\Delta w_{,xx}\mathrm{d}x\right] = \\ & = -\int_0^L \left[\mu\ddot{\overline{w}} + M^*_{,xx}\right]\Delta\dot{w}\mathrm{d}x + M^*_{,x}(L)\Delta\dot{w}(L) - M^*(L)\Delta\dot{w}_{,x}(L) . \end{aligned} \tag{2}$$

Provided the deviation of the deflection has homogenous initial conditions, then the left hand side of Eq. (2) is zero for the initial time. If we are further able to ensure the right hand side of Eq. (2) vanishes for all times, then the deviation of the deflection vanishes within the whole

beam for all times. An exact solution to this problem, which is denoted as dynamic shape control problem in the literature, is:

$$\begin{aligned} &M^*(x,t) = S(x)u(t) \\ &\text{with } u(t) = -\mu\ddot{\overline{w}}(t) \text{ and } S_{,xx} = 1, \quad x = L: \; S_{,x} = 0 \text{ and } S = 0\,. \end{aligned} \tag{3}$$

For a review on the method of shape control, see Irschik [4]. The solution of Eq. (3) requires the time variation of the support motion to be known. In general this will not be case. Then one needs to use methods of feedback control. The eigenstrain-type moment's span-wise distribution $S(x)$, the so-called shape function, can still be calculated from Eq. (3), but the time variation $u(t)$ should be provided be a controller, which is fed by a sensor signal. We seek to design a sensor, which is collocated to the eigenstrain-type moment, hence to the actuation. The power of this latter actuation with respect to the deviation of the deflection can be written as, see Eq. (2),

$$L^{(a)} = -\int_0^L M^* \Delta\dot{w}_{,xx}\mathrm{d}x = -u(t)\underbrace{\int_0^L S(x)\Delta\dot{w}_{,xx}\mathrm{d}x}_{=-\dot{y}(t)} = u(t)\dot{y}(t)\,. \tag{4}$$

The sensor signal $y(t)$ defined in Eq. (4) is the so-called natural output of the system, see Nijmeijer and van der Schaft [5], and it measures a weighted average of the curvature of the total deflection, because the curvature of the support motion is identically zero. The weighing function is identical to the span-wise distribution of the actuation and, therefore, actuation and sensing are collocated. We construct a closed loop system by exemplarily using a PD-controller, $u(t) = -Py(t) - D\dot{y}(t)$. For the free closed loop system we find the following statement from Eq. (2):

$$\frac{\mathrm{d}}{\mathrm{d}t}\left[\frac{1}{2}\int_0^L \mu\Delta\dot{w}\Delta\dot{w}\mathrm{d}x + \frac{1}{2}\int_0^L D\Delta w_{,xx}\Delta w_{,xx}\mathrm{d}x + \frac{1}{2}Py(t)y(t)\right] = -D\dot{y}(t)\dot{y}(t)\,. \tag{5}$$

Although Eq. (5) does not proof the stability of the closed loop system in the sense of Liapunov, but we consider it to be sufficient for establishing stability in this paper. For a proof of the stability of a cantilever with piezoelectric actuation and sensing, see Kugi [6] and Kugi et al. [7]. A detailed discussion on the design of collocated actuators and sensors for beams with application to the feedback control of sub-sections of beams can be found in Krommer and Nader [8]. In this section we shortly introduced the idea of dynamic shape control to eliminate flexural vibrations of a cantilever, which arise due and in addition to a given support motion. If the time variation of the support motion is known an exact elimination can be achieved by the method of dynamic shape control. If the time variation is unknown, dynamic shape control is still a useful tool, as it allows us to design collocated actuators and sensors, which can be used in feedback control to control the deviation of the deflection. In the next sections we will present analytical and numerical results, which show the power of the proposed method for the control of flexural vibrations superposed upon rigid body motions due to support motions.

SIMULATION OF THE DISCRETIZED ACTUATION

The continuous shape function of the eigenstrain-type moment according to Eq. (3) is approximated by means of a discrete piezoelectric patch actuation. The required amount of electric voltage and the spatial distribution of the discrete patches are determined according to the equal-area rule; i.e. it is chosen such that the area under the discretized function matches the area under the continuous distribution in Eq. (3). In the present case study, and from the experiences gained in Ref. [9], ten patches are used, where the positions of the patches are determined by the formula

$$x_{patch} = L(1 - \frac{k}{n})^{1.45}. \tag{6}$$

In Eq. (6), $n = 10$ is the total number of the patches and k is the number of the patch under consideration. The middle layer of the beam is made of aluminum, with a length $L = 500$ mm, width $b = 40$ mm and thickness $h_a = 4$ mm, Young's modulus $Y_a = 50 \cdot 10^9$ N/m^2, Poisson's ratio $\nu_a = 0.34$ and mass density $\rho_a = 2700$ kg/m^3. The two actuator layers are made of PZT-5A, each with a thickness of 0.35 mm. For the simulation the orthotropic material properties of PZT-5A are used, comprising a compliance of $S_{11} = 16.4 \cdot 10^{-12}$ m/N^2, a piezoelectric coefficient $d_{31} = -171$ pC/N and a density $\rho_p = 7750$ kg/m^3. The effective mass per unit length is given by $\mu = 0.649$ kg/m and the bending stiffness D results to 18.76 Nm^2.

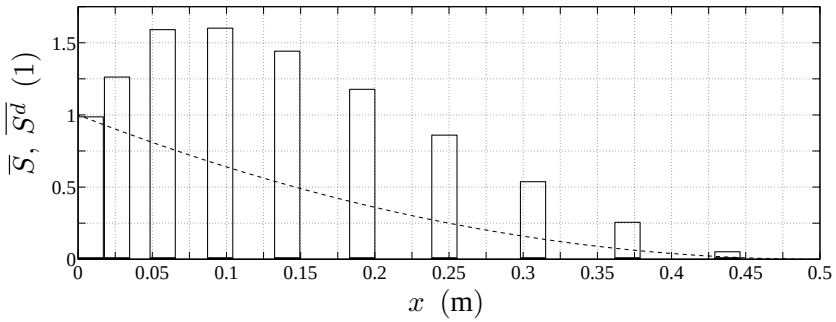

Figure 1: Shape function - dashed line: continuous. solid line: discretized.

Figure 1 shows the continuous and the discrete normalized shape functions $\overline{S}(x) = 2/L^2 S(x)$ and $\overline{S^d}(x) = 2/L^2 S^d(x)$. The area under the discrete electrode patches is chosen as equal to the area under the continuous shape function, not only in total, but also for partial areas.

For the purpose of simulation we have to approximate the infinite dimensional system by a finite dimensional one. Thus we expand the deflection into the eigenfunctions of the cantilever

$$\Delta w(x,t) = \sum_{i=1}^{n} \mathbf{W}^T(x)\, \mathbf{q}(t). \tag{7}$$

For the simulation, using the environment of MATLAB/Simulink, we use the state-space representation

$$\begin{bmatrix} \dot{\mathbf{q}} \\ \ddot{\mathbf{q}} \end{bmatrix} = \begin{bmatrix} \mathbf{0} & \mathbf{E} \\ -\mathbf{M}^{-1}\mathbf{K} & \mathbf{0} \end{bmatrix} \begin{bmatrix} \dot{\mathbf{q}} \\ \ddot{\mathbf{q}} \end{bmatrix} + \begin{bmatrix} \mathbf{0} \\ \mathbf{M}^{-1}\mathbf{s} \end{bmatrix} u + \begin{bmatrix} \mathbf{0} \\ \mathbf{M}^{-1}\mathbf{p} \end{bmatrix} d\,, \tag{8}$$

in which $d = \mu\ddot{\overline{w}}$ is the disturbance. The diagonal mass matrix $\mathbf{M}$, the diagonal stiffness matrix $\mathbf{K}$, the shape function vector $\mathbf{s}$ and the disturbance vector $\mathbf{p}$ are defined by

$$\mathbf{M} = \mu \int_0^L \mathbf{W}\mathbf{W}^T \mathrm{d}x = \mu\mathbf{E}\,, \quad \mathbf{K} = D \int_0^L \mathbf{W}''\mathbf{W}''^T \mathrm{d}x = D\, diag(\lambda_i^4)\,,$$
$$\mathbf{s} = -\int_0^L \mathbf{W}'' S^d \mathrm{d}x\,, \quad \mathbf{p} = -\int_0^L \mathbf{W}\mathrm{d}\mathbf{x}\,. \tag{9}$$

In the closed-loop simulation the parameters $P = 100$ and $D = 0.6$ are used for the PD-controller. Figure 2 represents two results for a 10^{th}-order model, showing the good performance of the vibration compensation under consideration.

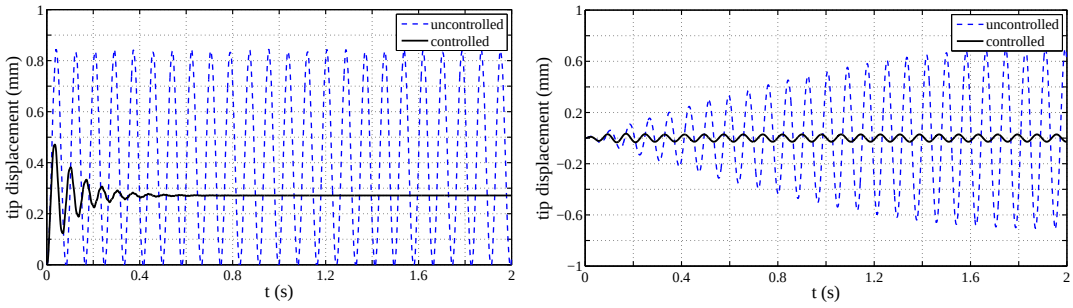

Figure 2: Step response and transient solution (excitation frequency at 12.3Hz).

FINITE ELEMENT COMPUTATIONS

The piezoelectric transducing mechanism is based on the interaction between the electric quantities, electric field intensity $\mathbf{E}$ and electric induction $\mathbf{D}$, with the mechanical quantities, mechanical stress tensor $[\boldsymbol{\sigma}]$ and strain tensor $[\mathbf{S}]$. By applying a mechanical load (force) to a piezoelectric transducer (e.g., piezoelectric material with top and bottom electrode), one can measure an electric voltage between the two electrodes (sensor effect). This mechanism is called the *direct piezoelectric effect*, and is due to a change in the electric polarization of the material. The so-called *inverse piezoelectric effect* is obtained by loading a piezoelectric transducer with an electric voltage. Therewith, the transducer will show mechanical deformations (actuator effect), and the setup can be used, e.g., in a positioning system. The material law describing the piezoelectric effect is given by

$$\boldsymbol{\sigma} = [\mathbf{c}^E]\mathbf{S} - [\mathbf{e}]^T\mathbf{E}\,, \tag{10}$$
$$\mathbf{D} = [\mathbf{e}]\mathbf{S} + [\boldsymbol{\varepsilon}^S]\mathbf{E}\,. \tag{11}$$

Since the stress tensor $[\boldsymbol{\sigma}]$ as well as strain tensor $[\mathbf{S}]$ are symmetric, it is convenient to write them as vectors of six components (the three normal and the three shear components) using

Voigt notation and denote them by $\boldsymbol{\sigma}$ and $\mathbf{S}$ [10]. The material tensors $[\mathbf{c}^E]$, $[\boldsymbol{\varepsilon}^S]$, and $[\mathbf{e}]$ appearing in Eq. (10) and Eq. (11) are the tensor of elastic modulus, of dielectric constants, and of piezoelectric moduli, respectively. The superscripts E and S indicate that the corresponding material parameters have to be determined at constant electric field intensity $\mathbf{E}$ and at constant mechanical strain $\mathbf{S}$, respectively. For deriving the coupled PDEs for piezoelectricity, we start at the local form of balance of linear momentum

$$\mathbf{f}_{\mathrm{V}} + \mathcal{B}^T \boldsymbol{\sigma} = \rho \ddot{\mathbf{u}}\,, \tag{12}$$

describing the mechanical field. In Eq. (12) $\mathbf{f}_{\mathrm{V}}$ denotes any mechanical volume force, ρ the density, $\mathbf{u}$ the mechanical displacement and $\mathcal{B}$ a differential operator, which computes as follows

$$\mathcal{B} = \begin{pmatrix} \frac{\partial}{\partial x} & 0 & 0 & 0 & \frac{\partial}{\partial z} & \frac{\partial}{\partial y} \\ 0 & \frac{\partial}{\partial y} & 0 & \frac{\partial}{\partial z} & 0 & \frac{\partial}{\partial x} \\ 0 & 0 & \frac{\partial}{\partial z} & \frac{\partial}{\partial y} & \frac{\partial}{\partial x} & 0 \end{pmatrix}^T . \tag{13}$$

Expressing $\boldsymbol{\sigma}$ by Eq. (10) and in-cooperating the strain–displacement relation

$$\mathbf{S} = \mathcal{B}\mathbf{u} \tag{14}$$

results in

$$\rho\ddot{\mathbf{u}} - \mathcal{B}^T \left([\mathbf{c}^E]\mathcal{B}\mathbf{u} - [\mathbf{e}]^T \mathbf{E} \right) = \mathbf{f}_{\mathrm{V}}\,. \tag{15}$$

Since piezoelectric materials are insulating, i.e., do not contain free-volume charges, and we do not have to consider any magnetic field, the electric field is determined by

$$\boldsymbol{\nabla} \cdot \mathbf{D} = 0 \text{ and } \boldsymbol{\nabla} \times \mathbf{E} = 0\,. \tag{16}$$

According to Eq. (16) we can express the electric field intensity $\mathbf{E}$ by the gradient of the scalar electric potential V_{e}

$$\mathbf{E} = -\boldsymbol{\nabla} V_{\mathrm{e}} = -\tilde{\mathcal{B}} V_{\mathrm{e}} \quad \text{with} \quad \tilde{\mathcal{B}} = (\partial/\partial x,\, \partial/\partial y,\, \partial/\partial z)^T\,. \tag{17}$$

By combining these results with Eq. (11) we obtain

$$\tilde{\mathcal{B}}^T \left([\mathbf{e}]\mathcal{B}\mathbf{u} - [\boldsymbol{\varepsilon}^S]\tilde{\mathcal{B}} V_{\mathrm{e}} \right) = 0\,. \tag{18}$$

Therefore, the describing partial differential equations for linear piezoelectricity read as

$$\rho\ddot{\mathbf{u}} - \mathcal{B}^T \left([\mathbf{c}^E]\mathcal{B}\mathbf{u} + [\mathbf{e}]^T \tilde{\mathcal{B}} V_{\mathrm{e}} \right) = \mathbf{f}_{\mathrm{V}}, \tag{19}$$

$$\tilde{\mathcal{B}}^T \left([\mathbf{e}]\mathcal{B}\mathbf{u} - [\boldsymbol{\varepsilon}^S]\tilde{\mathcal{B}} V_{\mathrm{e}} \right) = 0\,. \tag{20}$$

Applying the Finite-Element-Method (FEM) as described e.g. in [11], we arrive at the following semidiscrete Galerkin formulation

$$\begin{pmatrix} \mathbf{M}_u & 0 \\ 0 & 0 \end{pmatrix} \begin{pmatrix} \ddot{\underline{u}} \\ \ddot{\underline{V}}_{\mathrm{e}} \end{pmatrix} + \begin{pmatrix} \mathbf{C}_u & 0 \\ 0 & 0 \end{pmatrix} \begin{pmatrix} \dot{\underline{u}} \\ \dot{\underline{V}}_{\mathrm{e}} \end{pmatrix} + \\ + \begin{pmatrix} \mathbf{K}_u & \mathbf{K}_{uV} \\ \mathbf{K}_{uV}^T & -\mathbf{K}_V \end{pmatrix} \begin{pmatrix} \underline{u} \\ \underline{V}_{\mathrm{e}} \end{pmatrix} = \begin{pmatrix} \underline{\mathbf{f}_{\mathrm{V}}} \\ 0 \end{pmatrix}. \tag{21}$$

In Eq. (21) $\mathbf{M}_u$ denotes the mechanical mass matrix, $\mathbf{K}_u$ the mechanical stiffness matrix, $\mathbf{K}_V$ the electric stiffness matrix, $\mathbf{K}_{uV}$ the coupling matrix and $\underline{\mathbf{f}_V}$ the nodal mechanical forces. In addition, we have introduced the mechanical damping matrix $\mathbf{C}_u$, which we compute according to Rayleigh's damping model (see e.g. [12]). The time discretization is performed by applying the implicit Newmark scheme as described in [12]. The above described scheme is implemented in the simulation tool CFS++ [13], which is an enhanced Finite-Element-program for coupled field problems. The software allows a steering with Tcl-scripts, so that the Tcl-script has access to all simulation results as well as can set boundary condition, loads, etc. Therewith, the controller-structure is implemented in a Tcl-script, which steers the whole simulation. For a detailed description of digital controller design see e.g. Gausch, Hofer and Schlacher [14].

The whole structure has been discretized by 396 hexahedral finite elements resulting in a total number of 8.608 unknowns. We have chosen second order finite elements in order to avoid the well known locking effect in thin structures. The whole structure is excited by applying a prescribed movement of the left end of the beam with an amplitude of $10\,\mu$m and a frequency of 12 Hz, which corresponds to the first eigenfrequency. In order to test the performance of our controller, we have performed a transient analysis. Figure 3 displays the tip displacement of the beam, once without the controller (piezoelectric actuators being hot-wired) and once with the controller. Within the controller we have limited the maximum control voltage to 5 V.

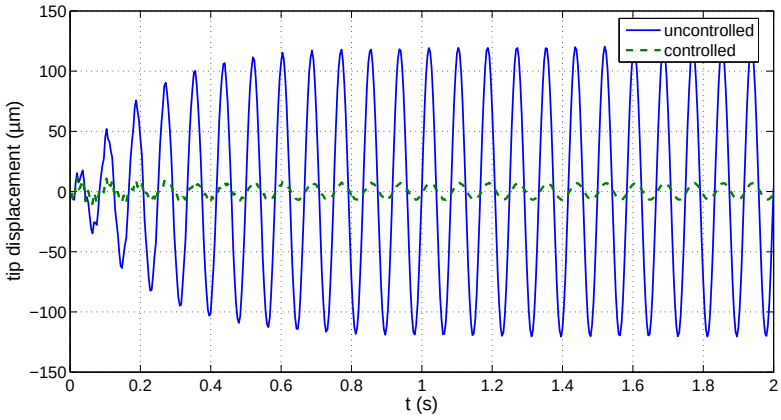

Figure 3: Tip displacement of the beam with and without the controller.

ACKNOWLEDGMENTS

The present paper is a contribution to the Linz Center of Competence in Mechatronics (LCM). Support of this center in the framework of the Austrian K+ Science Fund is gratefully acknowledged. The authors are grateful to Professor Hans Meixner and his group, Siemens Zentrale Technik München, for initiating this work, and for participating in the LCM.

References

[1] H. Irschik, M. Krommer, U. Pichler, *Dynamic shape control of beam-type structures by piezoelectric actuation and sensing*, International Journal of Applied Electromagnetics and Mechanics, 17, (2003), 251–258.

[2] M. Nader, H. Gattringer, M. Krommer, H. Irschik, *Shape control of flexural vibrations of circular plates by shaped piezoelectric actuation*, Journal of Vibration and Acoustics, 125(1), (2003), 88–94.

[3] F. Ziegler, *Mechanics of Solids and Fluids*, 2nd english edition, 2nd corrected printing, Springer, New York (1998).

[4] H. Irschik, *A review on static and dynamic shape control of structures by piezoelectric actuation*, Journal of Engineering Structures, 24, (2002), 5–11.

[5] H. Nijmeijer, A. J. van der Schaft, *Nonlinear Dynamical Control Systems*, Springer, New York (1991).

[6] A. Kugi, *Non-linear Control Based on Physical Models*, Springer-Verlag, London (2001).

[7] A. Kugi, D. Thull, K. Kuhnen, *An infinite-dimensional control concept for piezoelectric structures with complex hysteresis*, In print (available online): Journal of Structural Control and Health Monitoring.

[8] M. Krommer, M. Nader, *Collocated actuator / sensor design fo shape control of subregions of structures*, in R. C. Smith, ed., *Proceedings of SPIEs 11th Annual International Symposium on Smart Structures and Materials: Modeling, Signal Processing, and Control*, vol. 5383, San Diego, USA (2004), pp. 232 – 243.

[9] M. Nader, H.-G. v. Garßen, H. Irschik, *Vibration compensation of slender beams and thin shell structures by distributed piezoelectric patches*, in R. Flesch, H. Irschik, M. Krommer, eds., *Schriftenreihe der Technischen Universität Wien, Proceedings of the Third European Conference on Structural Control (3ECSC)*, vol. II, Technische Universität Wien, Vienna, Austria (2004), pp. S1–155 – S1–158.

[10] T. Belytschko, W. K. Lui, B. Moran, *Nonlinear Finite Elements for Continua and Structures*, Wiley (2000).

[11] M. Kaltenbacher, *Numerical Simulation of Mechatronic Sensors and Actuators*, Springer Berlin-Heidelberg-New York (2004).

[12] T. J. R. Hughes, *The Finite Element Method*, Prentice-Hall, New Jersey (1987).

[13] M. Kaltenbacher, A. Hauck, M. Mohr, E. Zhelezina, *CFS++: Coupled Field Simulation*, LSE, University of Erlangen (2005).

[14] F. Gausch, A. Hofer, K. Schlacher, *Digitale Regelkreise*, Oldenburgverlag (1993).